Microgravity Sci. Technol. manuscript No.
(will be inserted by the editor)

Analysis of characteristics of two-layer convective flows with diffusive type evaporation based on exact solutions

V. B. Bekezhanova[1,2] · **O. N. Goncharova**[3]

Received: date / Accepted: date

Abstract The theoretical approaches for mathematical modelling of the convective flows with mass transfer through the liquid – gas interface are discussed. The special attention is payed to modelling with use of the classical Boussinesq approximation of the Navier – Stokes equations. The diffusion equation and the effects of thermodiffusion and thermal diffusivity (the Soret and Dufour effects) are taken into account additionally to describe vapor and heat transfer processes in the gas-vapor phase. The use of the Oberbeck – Boussinesq equations allows one to apply the group-analytical methods in the theory of the evaporative convection and to construct the exact solutions of special type of the governing equations. Joint flows of the evaporating liquid and gas-vapor mixture are studied with the help of a partially invariant solution for the convection equations. The 2D and 3D solutions are demonstrated to simulate two-phase flows in the infinite channels with interface being under action of a longitudinal temperature gradient and perpendicularly directed gravity field. In the present paper the fluid flows with diffusive evaporation/condensation in the terrestrial and microgravity conditions are studied in the stationary case. The new results obtained for combined thermal regime on the external rigid boundaries are presented.

Keywords Thermocapillary convection · Phase transition · Evaporative convection · Mathematical model · Exact solution · Two-layer flow

PACS 02.60.Cb · 05.60.-k · 02.70.-c

Mathematics Subject Classification (2000) MSC 76T10 · 76R99

This work was partially supported by the Russian Foundation for Basic Research (project No. 17-08-00291, analysis of the evaporative convection regimes in 2D case) and by the Russian Foundation for Basic Research and the government of Krasnoyarsk region (project No. 18-41-242005, study of 3D flows).

[1] Department of Differential Equations of Mechanics, Institute of Computational Modelling SB RAS, 660036, Akademgorodok, 50/44, Krasnoyarsk, Russia
E-mail: vbek@icm.krasn.ru ·
[2] Institute of Mathematics and Computer Science, Siberian Federal University, 660041, Svobodny, 79, Krasnoyarsk, Russia
[3] Altai State University, 656049, pr Lenina 61, Barnaul, Russia
E-mail: gon@math.asu.ru

1 Introduction

1.1 Theoretical approaches for description of evaporation processes

The need for theoretical study of problems with evaporation or condensation is usually caused by extensive use of vapor-liquid environments in manufacturing processes and industrial equipment. Theoretical results obtained in this area can be applied in the development of advanced technologies, where the evaporating liquids and/or gas-vapor compounds are used as working media. Such modern fluidic technologies are the possible alternative to enhance the effective parameters of cooling systems and thermostabilization technics of electronic devices or complex packages, and to modify setups using evaporators and condensers. In our case, physical experiments carried out in the frame of international MAP Evaporation project have played the motivating role for theoretical study and development of refined models of convection. Doing analytical investigation of liquid flows with phase transitions, it is necessary not only to elaborate new mathematical models, which adequately describe physical processes, but also to reveal the mechanisms of possible crisis phenomena, to determine capabilities to control arising regimes of the fluid motion, to specify the influence character of physicochemical factors on the flow structures and the evaporation/condensation effects, to estimate and to predict the experiment efficiency.

A serious experimental and theoretical basis for study of fluid dynamics problems with evaporation have been laid in the 19th century. Starting with the work of Lame and Clapeyron [1], where the problem of the liquid ball solidification was considered and the first rigorous formulation of the problem with the liquid – solid phase transition was given, these and later famous results (see [2–9] formed the outlines for development of modern approaches in the study of evaporative convection. In the experiments of the above cited authors the evaporation characteristics have been considered as the functions on working media flow rate and temperature, on system geometry and fluid properties.

With rising costs for experiments the significance and importance of theoretical investigations also increase. Theoretical methods involves the development of a mathematical model, finding or obtaining new exact solutions of governing equations or generalizing known ones, their physical interpretation and validation, and lastly, investigating the stability obtained solutions.

Let us distinguish two different approaches to describe the transfer processes of momentum and energy in the two-layer systems with evaporation. The first one implies consideration of these processes separately in each phase with appropriate coupling conditions at the interface (see, for example, [10, 11]). By implementation of such approach the Navier – Stokes equations are used, and at the interface the mechanical interaction, heat and mass transfer are taken into account. In works [10, 12] the interface deformation as a result of pressure drop is considered. Evaporation is described here as a diffusion process and, correspondingly, as the diffusion problem. It is necessary to note a contradiction between diffusion theory and low evaporation rate, that has been discussed in [13]. Second approach presupposes, that the phases are distributed one into another according to some law, and one or both phases are continuous. At this, equations that characterize behavior system are formulated for medium as a whole (see [14]).

In general case, there is a region near the interface, where the flows are not described by the Navier – Stokes equations [15]. In this area the non-equilibrium processes should be taken into account. The kinetic theory of gases gives one of the possible ways to correctly describe these phenomena. In this case the kinetic Boltzmann equation is solved. In conditions, when evaporation is close to the global equilibrium state characterized by pressure and temperature values p_0 and T_0, we have so-called "weak evaporation" [16, 17]. In that case it is possible to neglect the viscous dissipation and molecular kinetic energy of vapor in the energy and momentum balance equations.

When constructing the mathematical models for description of flows with evaporation a principal issue is the choice of a system of equations and formulation of general conditions on the interface, which should be based on conservation laws and should include the additional effects associated with phase transition. The most significant work, which gives a mathematical model to describe such processes, was presented by Margerit and co-authors [17]. It is based on classical principles of thermodynamics of irreversible processes. The kinetic equation Hertz – Knudsen is used to determine the mass evaporation rate J taken into account in the mass balance equation and in the condition that specifies the heat flux jump on the interface. The saturated vapor temperature is determined using the Clapeyron – Clausius equation. The mathematical model proposed in [18] is a simplification of the above mentioned model [17].

The feature of approach used in [19] is that it is not based on the Gibb's theory for interface description but on introduction of the concept of surface heat capacity. The following key provisions lie at the core of this model: the temperature continuity is not presupposed; the surface divergence of the interface velocity is assumed to be zero; the statistical rate theory is used to determine the evaporation mass flow rate. In [20] the interface conditions are formulated on the basis of integral conservation laws with use of the interface Gibbs theory when the surface tension coefficient is identified with surface specific free energy. The method of description the diffusion nature of evaporation is similar to the approach in [17] and the presence of surfactants on interface are additionally accepted in [20]. In [21–23] the free boundary kinematic, dynamic and energy conditions are generalized for the case with evaporation/condensation at the interface. In the later papers the kinetic theory is used for the mass evaporation rate determination similarly to [17], and the latent heat of evaporation is defined as a jump in internal energy. We do not cite here the works where the Knudsen theory is developed and the Knudsen layer is introduced as a strong discontinuity to describe the problems with a phase transition.

1.2 Exact solutions of the evaporative convection equations having the group nature

The most developed systematic approach to classification and obtaining of the solutions of the governing equations is related to application of the group analysis methods of differential equations. Ovsyannikov's work [24] laid the foundations of systematic study of the group properties of the differential equations of mechanics. The integer-valued characteristics of solutions (rank and defect of invariance) have been introduced by Ovsyannikov to perform a solution classification, and rather simple and effective algorithms have been proposed to obtain solutions. Invariant and partially invariant solutions of rank 1 and 2 are classified as the exact solutions of differential equations [25], widening set of solutions classically referred to "exact" ones (i. e. written in the form of perfect formulae, quadratures, series or special functions). Exact solutions that have a group nature are particularly valuable because they allow one to effectively study the fundamental and secondary features of the physical processes described by governing equations. The Navier – Stokes or Oberbeck – Boussinesq equations provide the natural symmetry properties of space – time and of spatial fluid movement implied in deriving these relations.

A temperature gradient arises in the liquid in the presence of evaporation/condensation. For the first time, in the framework of the Boussinesq approximation an exact solution describing convective flow of the two-layer liquid in the presence of a longitudinal temperature gradient and mass transfer through the interface was presented in [26]. Later the solution was generalized for case of the liquid – vapor-gas mixture system with a thermocapillary interface for 2D [27] and 3D [28] cases. The group nature of these solutions, that can be referred to as the Ostroumov – Birikh type solutions (see review in [23]), of their analogues and generalizations, including the unsteady case, was proved in [29] and [30].

The idea to use the exact Ostroumov – Birikh solution to model the joint liquid and gas flows with respect to evaporation processes at interface is resulted from analysis of the experimental results [31–33]. The measurement data on the mass flow rate of evaporating liquid from the liquid layer surface blown by dry or wet gas, as well as the results of quantitative measurements of the average velocities of the vortex structures and the interface temperature gradient were obtained. The experimental data became a starting point for analysis of the 2D and 3D generalizations of this solution, their properties and applicability to modelling real joint flows of evaporating liquid and gas-vapor flux in different conditions, including different boundary regimes for the vapor concentration and temperature [34,35], and conditions of low gravity [36,37].

2 Mathematical model of evaporative convection

2.1 Basic assumptions and governing equations

We study the stationary two-layer flows of a volatile liquid and vapor-gas mixture in the horizontal channel with solid walls (Fig. 1). The vapor is considered as a passive component in the gas. The heat and mass transfer in the system is described with the help of the Boussinesq approximation of the Navier – Stokes equations. The vapor transport in the gas is described by the diffusion equation, that is a result of the Fick laws and of a more general Maxwell – Stefan equation concerning diffusion in the multi-component systems. Note, that in contrast to liquid compounds the Fick laws can be applied for description of intermolecular diffusion of gases not only under low concentration of an admixture but also under modern one [38]. The velocity vectors $\mathbf{v}_i = (u_i, v_i, w_i)$, functions of pressure p_i (deviation of pressure p' from the hydrostatic one, $p = p' - \rho \mathbf{g} \cdot \mathbf{x}$, $\mathbf{x} = (x, y, z)$), temperature T_i and vapor concentration C satisfy the convection equations:

$$(\mathbf{v}_i \cdot \nabla)\mathbf{v}_i = -\frac{1}{\rho_i}\nabla p_i + \nu_i \Delta \mathbf{v}_i - \mathbf{g}(\beta_i T_i + \underline{\gamma C}), \tag{2.1}$$

$$\operatorname{div} \mathbf{v}_i = 0, \tag{2.2}$$

$$\mathbf{v}_i \cdot \nabla T_i = \chi_i(\Delta T_i + \underline{\delta \Delta C}), \tag{2.3}$$

$$\mathbf{v}_2 \cdot \nabla C = D(\Delta C + \alpha \Delta T_2). \tag{2.4}$$

Here the index i (subscript or superscript) is responsible for belonging to the lower liquid layer Ω_1 if $i = 1$, or to the upper gas-vapor layer Ω_2 if $i = 2$, ρ_i is density of i-th fluid, ν_i, β_i, χ_i are the kinematic viscosity, thermal expansion, heat diffusivity coefficients of the fluids, respectively. Parameters γ and D are the concentration coefficient of the gas density and the diffusion coefficient of vapor in the gas. The diffusive thermal conductivity and thermodiffusion effects are taken into account in the gas-vapor layer, and coefficients δ and α characterize the Dufour and Soret effects, respectively. Equation (2.4) and underlined terms in (2.1) and (2.3) are used to model the motion in the gas-vapor layer only.

The liquid and gas-vapor mixture have a common interface Γ that admits a mass transfer from liquid to gas phase due to evaporation or condensation. We will suppose that Γ is a weakly deformable boundary. Along the surface the thermocapillary forces act. It is

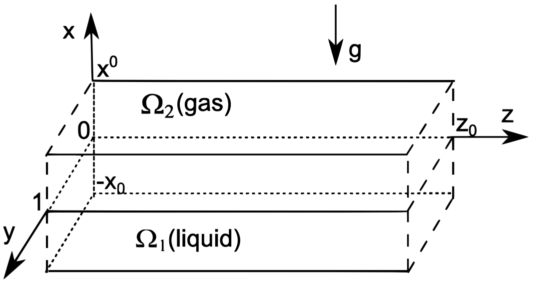

Fig. 1 Geometry of flow domain

assumed, that the surface tension σ linearly depends on the temperature T: $\sigma = \sigma_0 - \sigma_T(T - T_0)$; σ_0, T_0 are the reference values of the surface tension and liquid temperature, respectively, $\sigma_T > 0$ is the temperature coefficient of the surface tension. External boundaries of the system defined by equations $x = -x_0,\ x = x^0$ and $y = 0,\ y = 1$ are the rigid impermeable walls.

2.2 Boundary conditions

The required functions $\mathbf{v}_i$, p_i, T_i, C should provide correct description of the two-layer flows with interface in the channel with fixed boundaries, and satisfy not only the governing equations, but also definite additional relations. The following boundary conditions should be fulfilled on the boundaries. Relations on Γ contain the kinematic and dynamic conditions at thermocapillary surface, which in the stationary case can be written as follows:

$$\mathbf{v}_1 \cdot \mathbf{n} = \mathbf{v}_2 \cdot \mathbf{n} = 0, \tag{2.5}$$

$$(\mathbf{P}_1 - \mathbf{P}_2)\mathbf{n} = 2\sigma H \mathbf{n} + \nabla_\Gamma \sigma. \tag{2.6}$$

Here $\mathbf{n}$ is the unit vector of the external normal to Γ directed from domain Ω_1 into Ω_2, $\mathbf{P}_i = -p_i\mathbf{I} + 2\rho_i\nu_i\mathbf{D}(\mathbf{v}_i)$ is the stress tensor of i-th fluid, $\mathbf{D}(\mathbf{v}_i)$ is the velocity-strain tensor, H is the mean curvature of Γ (assume that $H > 0$ if the surface is bent outward relative to lower layer), ∇_Γ is the vector differential operator which denotes the surface gradient ($\nabla_\Gamma = \nabla - \mathbf{n}(\mathbf{n}\cdot\nabla)$). Projection of full dynamic condition (2.6) on the normal and two tangential vectors to the interface gives the following scalar relations:

$$\begin{gathered} -p_1 + p_2 + 2\big(\nu_1\rho_1\mathbf{D}(\mathbf{v}_1) - \nu_2\rho_2\mathbf{D}(\mathbf{v}_2)\big)\,\mathbf{n}\cdot\mathbf{n} = \\ = 2\sigma H, \end{gathered} \tag{2.7}$$

$$2\big(\nu_1\rho_1\mathbf{D}(\mathbf{v}_1) - \nu_2\rho_2\mathbf{D}(\mathbf{v}_2)\big)\,\mathbf{n}\cdot\mathbf{e}_{1,2} = \nabla_\Gamma\sigma\cdot\mathbf{e}_{1,2}.$$

Here, the vector triple $\mathbf{n}$, $\mathbf{e}_1$, $\mathbf{e}_2$ includes the normal (external relative to Ω_1) and tangential vectors at the interface. In the non-dimensional form the first condition in (2.7) is written as follows:

$$\begin{gathered} \mathrm{Ca}\,\big(-\ \mathrm{Re}(p_1 - p_2) + 2(\mathbf{D}(\mathbf{v}_1) - \rho\nu\mathbf{D}(\mathbf{v}_2))\big) = \\ = 2\sigma H, \end{gathered} \tag{2.7$'$}$$

where $\mathrm{Re} = u_* h/\nu_1$ is the Reynolds number, $\mathrm{Ca} = \rho_1\nu_1 u_*/\sigma_0$ is the capillary number, u_* is the characteristic velocity, h is the characteristic length, $\rho = \rho_2/\rho_1$, $\nu = \nu_2/\nu_1$. On the assumption of that Γ is a weakly deformable interface, or the same, the capillary number is small ($\mathrm{Ca} \ll 1$), the relations $H = 0$ and

$$-\,\mathrm{Re}(p_1 - p_2) + 2(\mathbf{D}(\mathbf{v}_1) - \rho\nu\mathbf{D}(\mathbf{v}_2)) = 0 \tag{2.7$''$}$$

are a leading term and a consequence of the first order term in the expansion of (2.7)$'$ in this small parameter, respectively. The first equality $H = 0$ means that the interface remains a flat surface defined here by $x = 0$.

The evaporation/condensation effects are taken into account only in the heat balance equation at interface similarly to [18]. The heat transfer condition with respect to the diffusive mass flux due to evaporation/condensation and the mass balance equation are formulated at the interface Γ in the form:

$$\kappa_1\frac{\partial T_1}{\partial n} - \kappa_2\frac{\partial T_2}{\partial n} - \delta\kappa_2\frac{\partial C}{\partial n} = -LM, \tag{2.8}$$

$$M = -D\rho_2\left(\frac{\partial C}{\partial n} + \alpha\,\frac{\partial T_2}{\partial n}\right). \tag{2.9}$$

Here κ_i is the heat conductivity coefficient, L is latent heat of evaporation, M is the evaporative mass flow. The function M is the qualitative characteristics that is indicative of specifity of the phase transition phenomena. If $M > 0$ then the liquid evaporation occurs, negative values of M correspond vapor condensation in the system. This parameter is introduced specially to define the relationship between the thermal and mass balance conditions at the interface. Besides, M is an additional quantitative parameter for comparing the analytical and experimental results.

Condition (2.8) takes into account evaporation of diffusive type, which is regarded as the weak evaporation occurring under the conditions of modern temperature drops. Note that requirement for modern temperature drop in the system provides a correct application of the Oberbeck – Boussinesq approximation in the problem under study.

The linearized form of an equation for saturated vapor concentration on the interface being a consequence of the Clapeyron – Clausius equation and Mendeleev – Clapeyron equation for an ideal gas is used [35]:

$$C\big|_\Gamma = C_*(1 + \varepsilon_*(T_2 - T_0)\big|_\Gamma). \tag{2.10}$$

Here C_* denotes the saturated vapor concentration at $T_2 = T_0$ (T_0 will be equal to 20^oC in this paper), $\varepsilon_* = L\mu/(R^* T_0^2)$, μ is the molar mass of the evaporating liquid, R^* is the universal gas constant.

The continuity conditions of the tangential velocities and temperature at Γ are set additionally:

$$\mathbf{v}_1 = \mathbf{v}_2, \quad T_1 = T_2. \tag{2.11}$$

In the present work we assume that the upper and lateral fixed walls of the channel at $x = x^0$, $y = 0$ and $y = 1$ to be thermal insulated, i. e. the following conditions are imposed for the temperature functions on these external boundaries

$$\frac{\partial T_2}{\partial n} + \delta \frac{\partial C}{\partial n} = 0. \tag{2.12}$$

But on the substrate at $x = -x_0$ the thermal load is applied according to linear law with respect to longitudinal coordinate:

$$T_1 = -A_1 z + T_{10}. \tag{2.13}$$

In (2.13) value A_1 defines a longitudinal temperature gradient and characterizes intensity of thermal load.

Conditions defining the boundary thermal regime can be various. All the boundaries can be heat-insulated and relations of form (2.12) should be set, upon that the longitudinal temperature gradient are formed only on the interface, as well as thermal load according to some law can be applied at all the external walls. The realization of these configurations in experimental setups is possible due to arrangement of a number of the thermoelectric modules of a small size on walls (in the first case these modules are placed on end wall of a long cuvette away from the test section). The elements can be operated independently of each other and to set various temperature.

The no-slip conditions for the velocity fields are fulfilled on all the external rigid boundaries of the system:

$$\mathbf{v}_i = 0. \tag{2.14}$$

In this paper we consider the case of absence of vapor flux on the walls at $x = x^0$ and partially at $y = 0$, $y = 1$:

$$\frac{\partial C}{\partial n} + \alpha \frac{\partial T_2}{\partial n} = 0. \tag{2.15}$$

It should be noted that another type of boundary conditions for vapor concentration on the upper and lateral rigid boundaries can be used, namely, zero vapor concentration condition $C = 0$. Characteristics of the two-layer flows with evaporation under different conditions for function of vapor concentration C have been studied in the 3D statement (see [35]).

3 Generalization of the Ostroumov – Birikh solution

3.1 General form of exact solution

Since further mathematical modelling will be based on exact solutions of the governing equations, we consider that an infinite channel located in transversely directed gravity field will be chosen for a canonical region: an infinite channel with a rectangular cross section in 3D case (see Fig. 1) and an infinite strip in 2D case (section of the 3D channel by a plane $y = 0$). Let the gravitational vector be directed opposite to the Ox axis ($\mathbf{g} = (-g, 0, 0)$). We consider two layers Ω_1 and Ω_2 in the 3D case (see Fig. 1)

$$\Omega_1 = \{(x, y, z) : -x_0 < x < 0, 0 < y < 1, -\infty < z < \infty\},$$

$$\Omega_2 = \{(x, y, z) : 0 < x < x^0, 0 < y < 1, -\infty < z < \infty\}$$

filled by a volatile liquid and gas-vapor mixture with an interface Γ; Γ is defined here by equation $x = 0$ and assumed to be nondeformed (flat) interface when constructing the exact solution (see consequences of the dynamic condition $(2.7)'$ in Subsection 2.2).

We construct the solution of system (2.1) – (2.4) as follows. The velocity vector components (u_i, v_i, w_i) depend on the transversal coordinates (x, y) only. Temperature, pressure and vapor concentration functions have summands Θ_i, q_i, Φ also depending on the transversal coordinates (x, y):

$$u_i = u_i(x, y), \quad v_i = v_i(x, y), \quad w_i = w_i(x, y), \tag{3.1}$$

$$p_i = -A\,\rho_i \beta_i g\,xz + \delta_i^2 B \rho_2 \gamma\, g\,xz + q_i(x, y), \tag{3.2}$$

$$T_i = -Az + \Theta_i(x, y), \tag{3.3}$$

$$C = Bz + \Phi(x, y). \tag{3.4}$$

This solution is the partially invariant solution of rank 2 and defect 3 and can be referred to as an “exact” solution in the comprehensive sense [25]. Coefficients A and B specify the constant longitudinal gradients of the temperature and vapor concentration along the interface; δ_i^2 is the Kronecker delta. Presented solution is the generalization of the Ostroumov – Birikh solution for thermoconcentration convection equations.

We interpret solution (3.1) – (3.4) as a solution describing the three-dimensional flow with the phase transition in the working area $[0, z_0]$ in a sufficiently long cavity. Structure of the exact solution provides preservation of the flow topology in any two cross-sections z_1, z_2 since the velocity components do not depend on the longitudinal coordinate. Furthermore, the solution satisfies exactly all the governing equations and boundary conditions on the interface, and it does not presuppose an axial symmetry.

3.2 2D analogue of the exact solution

Due to the group properties of system (2.1) – (2.4) three-dimensional solution (3.1) – (3.4) has two-dimensional analogue. The 2D solution are characterized by the linear dependence of the temperature, vapor concentration and pressure functions on the longitudinal coordinate z; only the longitudinal components of velocity are not equal to zero and depend on the transverse coordinate x:

$$\begin{aligned} &u_i = 0,\ w_i = w_i(x),\ p_i = p_i(x,z),\\ &T_i = (a_1^i + a_2^i x)z + \vartheta_i(x),\ C = (b_1 + b_2 x)z + \phi(x). \end{aligned} \tag{3.5}$$

It possesses an invariant property with respect to group of transformations ∂_t, ∂_y and $Z = -A^{-1}\partial_z + \rho\beta g x \partial_p + \partial_T - \rho_2\gamma(B/A)gx\partial_{p_2} - (B/A)\partial_C$ and, therefore, it is solution of rank 1 and defect 3. Exact expressions for unknown functions are defined easily as a result of substitution of relations (3.5) into the governing equations. All the required functions are presented in the polinomial form:

$$w_i = L_4^i x^4 + L_3^i x^3 + \frac{c_1^i}{2}x^2 + c_2^i x + c_3^i, \tag{3.6}$$

$$\begin{aligned} T_i = {} & (a_1^i + a_2^i x)z + N_7^i x^7 + N_6^i x^6 + N_5^i x^5 + N_4^i x^4 +\\ & + N_3^i x^3 + N_2^i x^2 + c_4^i x + c_5^i, \end{aligned} \tag{3.7}$$

$$\begin{aligned} C = {} & (b_1 + b_2 x)z + S_7 x^7 + S_6 x^6 + S_5 x^5 + S_4 x^4 +\\ & + S_3 x^3 + S_2 x^2 + c_6^2 x + c_7^2, \end{aligned} \tag{3.8}$$

$$\begin{aligned} p_i = {} & \left[d_3^i \frac{x^2}{2} + d_2^i x + d_1^i\right] z +\\ & + K_8^i x^8 + K_7^i x^7 + K_6^i x^6 + K_5^i x^5 + K_4^i x^4 + K_3^i x^3 +\\ & + K_2^i x^2 + K_1^i x + c_8^i. \end{aligned} \tag{3.9}$$

The coefficients L_k^i, N_j^i, S_j^i, K_l^i ($i = 1,2$; $k = 3,4$; $j = 2,...,7$; $l = 1,...,8$) are expressed through the physical parameters, solution coefficients a_m^i, b_m ($i,m = 1,2$) and integration constants c_l^i ($i = 1,2$; $l = 1,...8$). The exact expressions for these coefficients are presented in [39]. All the unknown integration constants c_l^i are determined by the boundary conditions. The solution parameters b_1, b_2, a_1^i, a_2^i also satisfy certain relations imposed by the boundary conditions. The temperature continuity condition in (2.11) leads to the relations $a_1^1 = a_1^2 = A$. To uniquely determine all the constants in the frame of 2D formulation it is necessary establish an additional condition. To correctly close the problem statement the mass flow rate of the gas is set

$$Q = \int\limits_0^{h_2} \rho_2 u_2\,(x)\ dx. \tag{3.10}$$

When choosing the additional closing condition we take into account the configuration of real experimental setup that allows to control a flow rate both of a gas/vapor-gas mixture and a liquid.

Algorithm of finding all the integration constants and solution parameters in the case of boundary conditions (2.12) and (2.13) for the temperature functions is given in Appendix 1.

Structure of solution (3.5) allows one to use different types of boundary conditions for the temperature functions. In the framework of the 2D problems the characteristics of the two-layer flows with evaporation/condenstaion described by (3.5) have been studied most completely for the case, when the linear in the longitudinal coordinate distribution of the temperature on both external walls is set (see works cited in Subsection 2). Case of combined thermal regime on the rigid wall has not been studied systematically yet. In [40] the applicability of the Neumann boundary conditions for the temperature functions have been discussed, and some characteristics of the flows have been presented.

3.3 Determination of the required functions in the 3D case

Form of solution (3.1) – (3.4) allows one to reduce the original three-dimensional problem to the chain of two-dimensional problems for finding the unknown functions (here u_i, v_i, w_i, Θ_i, Φ). In this case the analytical research should be complemented by numerical investigations (in comparison with the 2D case, when the exact solution construction is carried out fully analytically). The reduction procedure of the 3D problem to a set of two-dimensional ones is specified in [35]. The 2D problems are solved numerically with the help of the developed numerical algorithm and with use of the author's code. Numerical algorithm is based on the longitudinal transverse finite difference scheme of second order approximation being unconditionally stable. Computation of q_i functions will not be needed because of reformulation of problems for transverse velocity components in terms of new functions, which are the third components of the vector potential and rotor of velocity. Description of the general scheme of numerical realization to model the 3D convective two-layer flows with evaporation at the interface on the basis of solution (3.1) – (3.4) is given in [35] (some additional details for this numerical algorithm are given in [37]).

4 Characteristics of flow regimes

4.1 Plane case

The 2D stationary solutions of type (3.5), that describe the convective flows with evaporation, allowed one to extend the Napolitano classification [41] for flows arising in two-layer systems with the themocapillary interface. In deriving the classification, the processes of mass transfer through the interface were not taken into account. Napolitano singled out the flows of the purely thermocapillary, mixed and Poiseuille's flow types, depending on the dominant effects that define the typical velocity profiles in the system.

We specified the same three classes of flows, analyzing types of the currents that occurs in a plane channel with rigid walls subjected to thermal load distributed by linear law of the form (2.13) on each solid boundary:

$$T_i = -A_i z + T_{i0}. \tag{4.1}$$

Here, if $i = 1$ or $i = 2$ then last condition sets thermal regime on the lower ($x = -x_0$) or upper ($x = x^0$) wall, respectively. In general case different thermal load can be applied on the external boundaries (with various gradients A_i and terms T_{i0}). If the thermocapillary effect is a main mechanism of the motion and dominate over other factors, then the purely thermocapillary flow with a fully return movement in the liquid phase will be realized. Mixed flow is characterized by a splitting of the velocity profile near the interface. The "layering" is caused by interaction of the tangential and thermocapillary forces. The Poiseuille flow will be realized with velocity profile close to parabolic one in both phases (liquid and gas), when the thermocapillary mechanism is suppressed by others (gravity force or significant tangential stresses due to quite large gas flow rate). The flow types are observed independently of the boundary regime type for the vapor concentration function (both zero vapor flux and zero vapor concentration conditions can be imposed). Essential feature of the flows with evaporation/condensation is that in the classification of flow regimes which can be described using exact solution (3.5), one should take into account not only the velocity profile structure but also the temperature distribution in the system. In case when conditions of form (4.1) on both walls are set a combined action of the thermocapillary effect and evaporation can leads to formation of a thermal field with non-uniform temperature gradients in the transverse direction. As a result, in the system the regimes with a thermocline near the interface or within the liquid, as well as regimes with inclined temperature gradient can appear [42,43].

As pointed out above, solution (3.5) admits realization of the flow with different temperature gradients A_i on the walls and non-zero transverse temperature drop when $T_{10} \neq T_{20}$. Upon that a resulting gradient A on the interface is formed. Its value is determined by special conditions of constraint and depends on values of A_i, geometry system (fluid layer thicknesses), thermal properties of the media and the inclusion/exception of the thermodiffusion effects [34,43]. In general case three subtypes of mixed flows are identified. The first type of mixed flow (mixed flow I) is characterized by a velocity profile stratification near the interface and the emergence of zones with a return current near the interface. The main flow mechanisms are the oppositely directed tangential stresses induced by the gas flux in the upper layer and thermocapillary forces. Mixed flows of the second type (mixed flow II) have a velocity profile stratification near the interface with a positive longitudinal component. Here the co-directed tangential stresses and thermocapillary forces are the main flow mechanism. Third type mixed flow (mixed flow III) is defined by the structure of the velocity field close to the Couette profile in one of the phases or simultaneously in both.

Under different thermal load applied on the walls there are three subclasses among the Poiseuille's type flows. The first class or classical purely Poiseuille's flow (Poiseuille's flow I) found also by Napolitano includes the regimes with velocity profiles that are close to parabolic ones in the fluids. The Poiseuille's flow I is characterized by positive values of the longitudinal velocity in each phase, and the pressure gradients are the main flow mechanisms. The second class or the first type conditionally Poiseuille's flow (Poiseuille's flow II) is distinguished by formation of reverse movement in the near wall area in one of the layers. The pressure gradients and viscous forces are the main flow mechanisms. Regimes where the liquid is in the rest state due to the thermocapillary effect and the velocity profile in gas is close to parabolic one refer to the third class or the second type conditionally Poiseuille's flow (Poiseuille's flow III). Here the thermocapillary effect and tangential stresses induced by co-current gas flux are the main and competing mechanisms. It is emphasized that mixed flows of the second type, as well as the conditionally Poiseuille's flows of both types, can appear only under conditions of different thermal loads applied on the outer channel walls (at different values of longitudinal temperature gradients prescribed at the rigid boundaries).

This expansion of the Napolitano classification for motion types was obtained for the case when conditions of form (4.1) on both walls were fulfilled. If the combined thermal regime on the rigid boundaries is set (i. e. conditions (2.12) and (2.13) are imposed), then all the

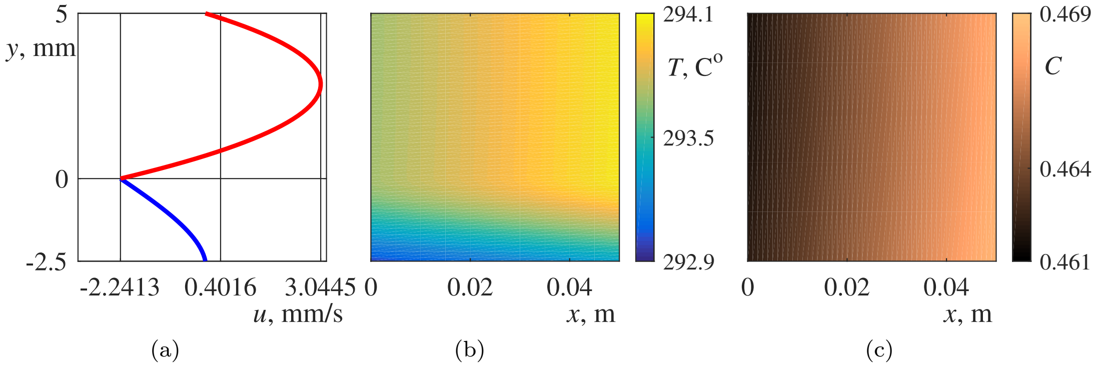

Fig. 2 Distributions of the longitudinal velocity $w(x)$ (a), temperature $T(x,z)$ (b) and vapor concentration $C(x,z)$ (c) in the system with $A_1 = A = -7$ K/m under terrestrial gravity ($g = g_0 = 9.81$ m/s^2) at $x_0 = 2.5$ mm, $Q = 9.6 \cdot 10^{-6}$ kg/(m·s^2)

same subclasses of the flows can be realized. Examples of configurations with pure thermocapillary (Fig. 2), mixed (Fig. 3), and Poiseuille's (Fig. 4) flows are given for system like "HFE-7100 – nitrogen" with upper thermally insulated wall. In all cases the gas layer thickness x^0 and length of test section z_0 were chosen to be equal to $x^0 = 5$ mm and $z_0 = 5$ cm, respectively. The physico-chemical parameters of the media are presented in Appendix 2 [44]. In Figs. 3(a,d,g) profiles of velocity of mixed I, mixed II, mixed III flow types are shown, respectively, as well as Figs. 4(a,d,g) present profiles of Poiseuille's I, Poiseuille's II, Poiseuille's III flow types. Thus, the use of the different types of boundary conditions for the temperature functions does not lead to additional expansion of the Napolitano classification based only on the analysis of velocity field pattern in the system.

As for the structure of the temperature field one should note that thermal insulation of the upper boundary provides mostly conditions for formation of the temperature field that is uniform in the transversal direction with potentially stable (Figs. 2(b), 3(e,h), 4(e)) or unstable (Figs. 4(b,h)) temperature stratification. However, regimes with the thermocline (Fig. 3(b)) can appear in the considered case also. In this case in the system the domains with gravitationally stable and unstable stratification coexist, therefore, additional mechanisms of instability can appear.

4.2 Three-dimensional flows

Numerical investigations of the evaporative convection regimes on the basis of 3D solution of form (3.1) – (3.4) are carried out to compare the characteristics of possible regimes, obtained in the frame of 2D and 3D approaches, to understand impact of the third spatial dimension, and to elucidate feasibility of 2D solution for description of real physical flows.

We investigate the flow topology, distributions of the temperature in the channel and vapor concentration in the upper layer computed for the same system of working media and the same configurations (layer thicknesses, gravity field intensity, etc.) as for 2D case.

In the 3D pictures the fluid tube projections on the $z = 0$ and $z = 2.5$- cross-sections and trajectories of the fluid particles (Figs. 5(a,b), 6(a)), fields of temperature in the system (Figs. 5(c,d), 6(b)) and vapor concentration distribution in the gas layer (Figs. 5(e,f), 6(c)) are presented for several cases. Basic characteristics shown in Figs. 5, 6 correspond to configurations for the flows of the purely thermocapillary (Figs. 5(a,c,e)), mixed II (Figs. 5(b,d,f)) and Poiseuille's III (Fig. 6) types in 2D case.

The 3D solution allows us to describe the roll-type convection when ordered patterns with the centerlines directed along the longitudinal axis appear. Upon that the planforms of the flows, that are the projections of the fluid tubes on the (x,y)-plane, are changed depending on the character of the applied thermal load, gravity level, and liquid layer thickness (compare topological structure of the flows in Fig. 5(a,b), 6(a)). For considered cases the motion has mainly translatory character that is occasioned by the thermocapillary effect action. Rotational motion is just weak. In order to show a presence of the rotational component of the flows we multiply the first and second velocity components of the liquid by factor 10^5 for all the configurations under consideration. The fluid trajectories are rounded the fluid tubes along the channel. The Marangoni force induces a movement of the liquid from hot domain to cold one, thus direction of the motion in the subsurface depends on value of the temperature gradient A. But the thermocapillary effect can both dominate and

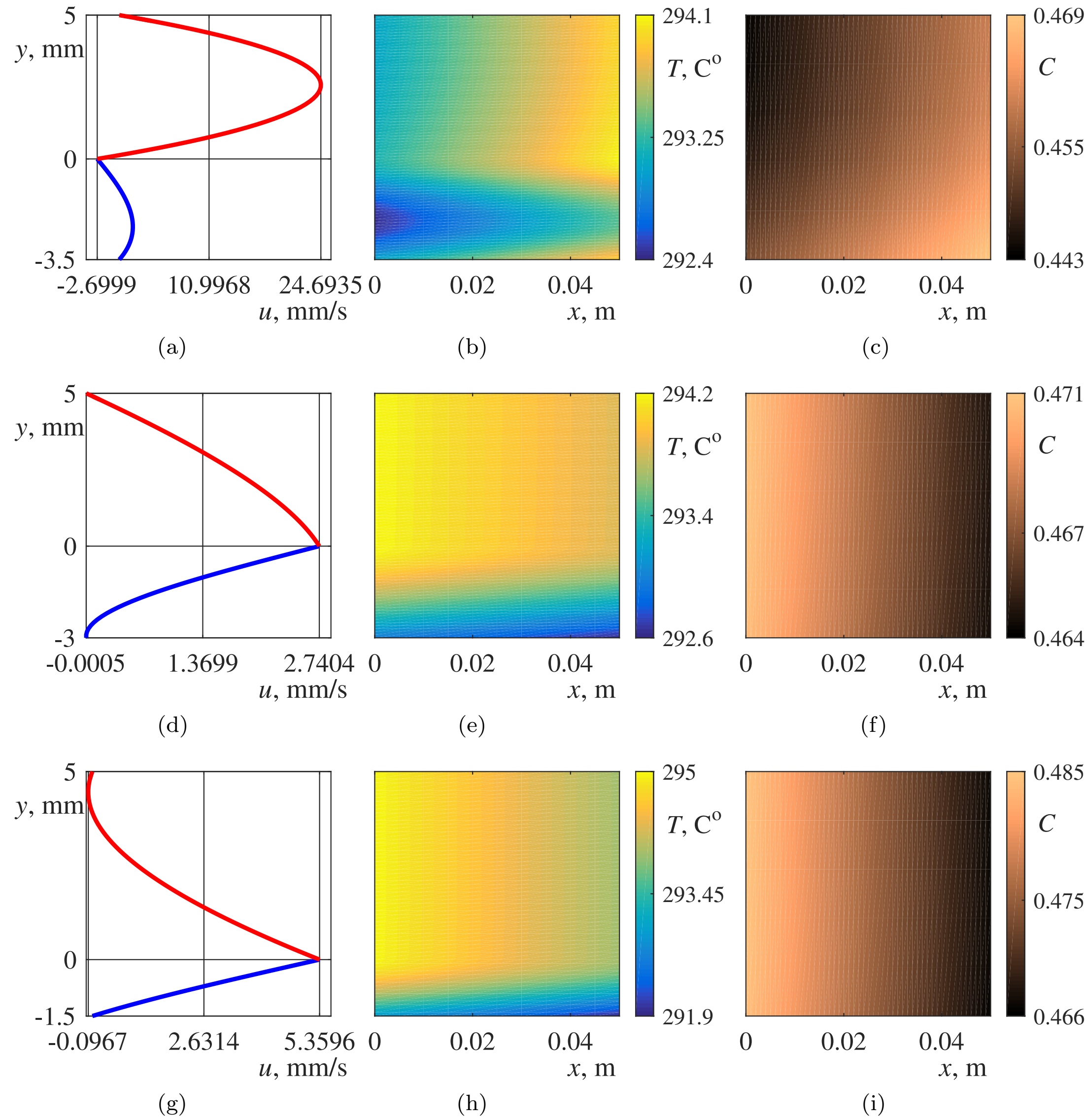

Fig. 3 Distributions of the longitudinal velocity $w(x)$ (a,d,g), temperature $T(x,z)$ (b,e,h) and vapor concentration $C(x,z)$ (c,f,i) in the system being under terrestrial gravity with $A_1 = A = -18$ K/m at $x_0 = 3.5$ mm, $Q = 9.6 \cdot 10^{-5}$ kg/(m·s^2) (a–c), with $A_1 = A = 7$ K/m at $x_0 = 3$ mm, $Q = 9.6 \cdot 10^{-6}$ kg/(m·s^2) (d–f), with $A_1 = A = 20$ K/m at $x_0 = 1.5$ mm, $Q = 9.6 \cdot 10^{-6}$ kg/(m·s^2) (g–i)

determine completely the hydrodynamical structure of arising regime and compete with other mechanisms. In the case corresponding to the purely thermocapillary flow a fully counter motion in the liquid is predicted by the 3D solution in exactly the same way as by its 2D analogue (compare Figs. 2(a) and 5(a)). The visualized trajectories in Fig. 5(a) are given for liquid particles with initial location at $z = 2$. Influence of rival mechanisms can be seen distinctly in Fig. 5(b) obtained for the case appropriate to the mixed flow II. The liquid motion is reverse at the bottom of liquid layer where liquid particles shift in the opposite direction of the z-axis, whereas near the interface the liquid moves to region with lower temperature (in the direction of z-axis). In the figure the trajectories are given for fluid particles with initial location at $z = 1$. The velocity profile presented in Fig. 3(d) for this flow type in the plane case forecasts similar topological pattern. It should be noted that in the 3D case a complication of spatial structure of the flow occurs in comparison with other configurations under consideration. The rolls are splitted into smaller shafts; "stratification" of the liquid is observed with formation of a two-layered roll-type structure. At this, defective rolls arise in the lower part of the liquid layer (compare planforms in Fig. 5(b) and in other cases). Any distortion of the regular form for the thermocap-

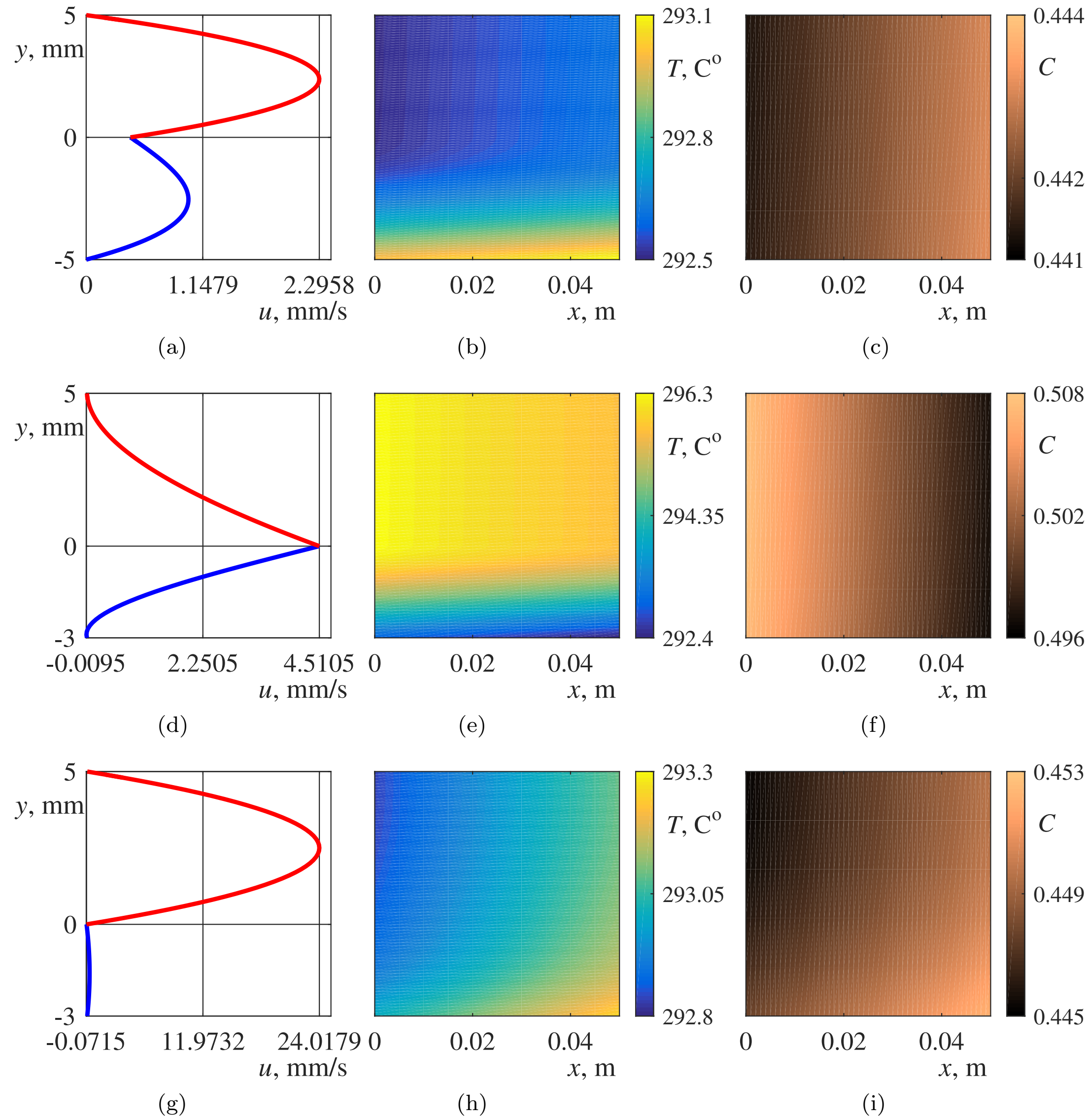

Fig. 4 Distributions of the longitudinal velocity $w(x)$ (a,d,g), temperature $T(x,z)$ (b,e,h) and vapor concentration $C(x,z)$ (c,f,i) in the system with $A_1 = A = -2$ K/m at $x_0 = 5$ mm, $Q = 9.6 \cdot 10^{-6}$ kg/(m·s^2), $g = g_0$ (a−c), with $A_1 = A = 5$ K/m at $x_0 = 5$ mm, $Q = 9.6 \cdot 10^{-6}$ kg/(m·s^2), $g = g_0$ (d−f), with $A_1 = A = -5$ K/m at $x_0 = 3$ mm, $Q = 9.6 \cdot 10^{-5}$ kg/(m·s^2), $g = g_0 \cdot 10^{-2}$ (g−i)

illary rolls points to a presence of a competitive mechanism. For the Poiseuille's III type flow an intensification of rotational movement takes place in the 3D case (compare liquid particle trajectories in Figs. 6(a) and 5(a,b)), whereas the 2D solution describes the regime with quiescent liquid. Impact of the transversal spatial dimensions is manifested in this way. Thus, alteration of the planforms, and consequently, of a spatial structure of the flows allows one to gauge a character and nature of influence of particular factors. But in the plane case the velocity profile gives qualitative information with respect to a possible topological structure of the two-layer flows.

As for thermal characteristics and vapor content for the two-layer flow regimes one can see that a good qualitative agreement between 2D and 3D distributions of the temperature and vapor concentration takes place. It suffices to compare the corresponding patterns of the temperature and vapor concentration fields for plane and three-dimensional configurations (Figs. 2(b),(c) and Figs. 5(c),(e) for the purely thermocapillary flow, Figs. 3(e),(f) and Figs. 5(d),(f) for the mixed type flow, and Figs. 4(h),(i) and Figs. 6(b),(c) for the Poiseuilles's flow), and one can conclude that the 2D solution predicts exactly structure of the thermal field and vapor content in the gas. Thus, we can forecast an appearance

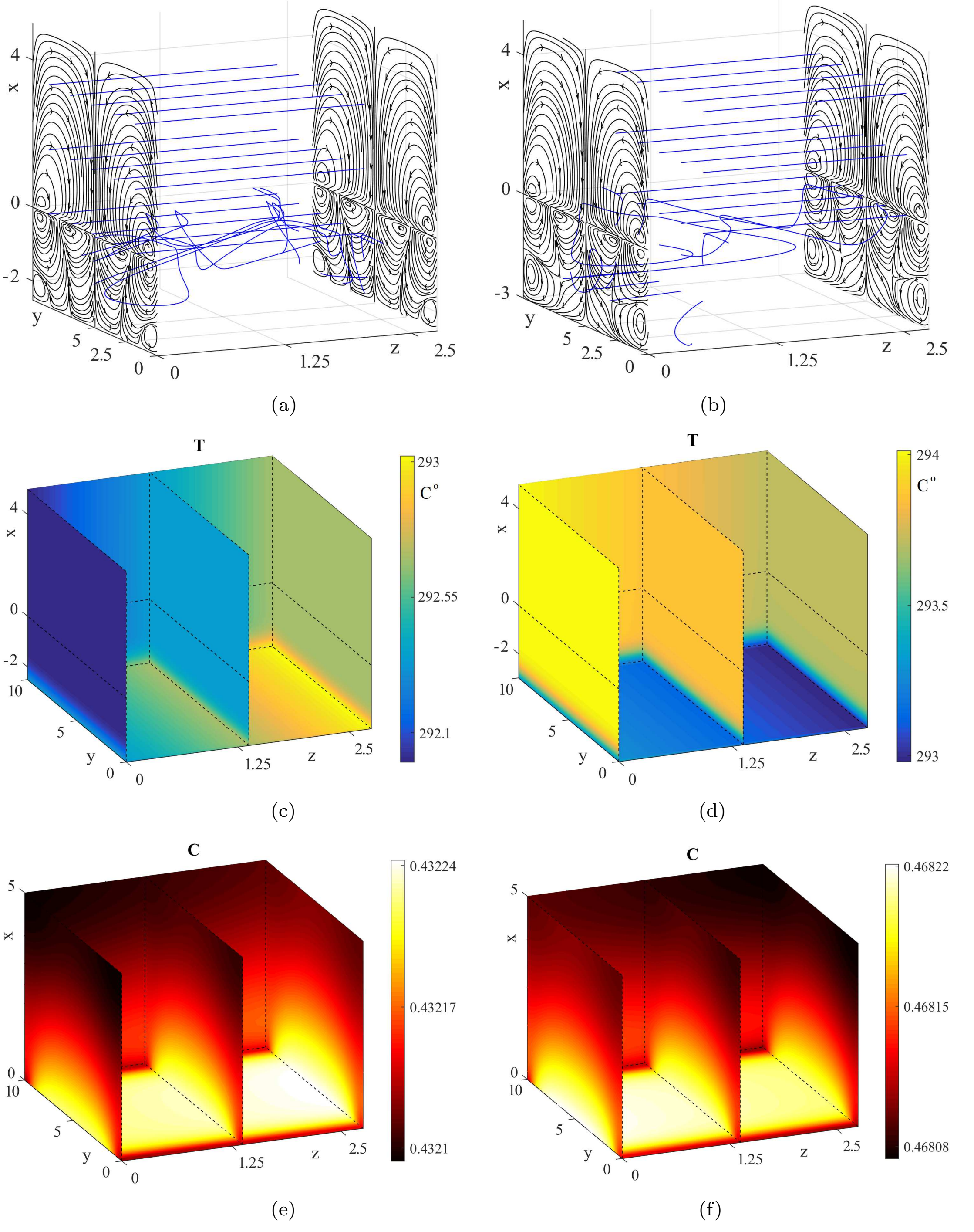

Fig. 5 Streamlines and trajectories (a,b), temperature (c,d) and vapor concentration (e,f) in the system being under terrestrial gravity ($g = g_0$) with $x_0 = 2.5$ mm, $A_1 = -7$ K/m (a,c,e); with $x_0 = 3$ mm, $A_1 = 7$ K/m (b,d,f)

of the regimes with potentially stable or unstable temperature stratification and evaluate parameters related to the evaporation/condensation effects (for example, mass flow rate) or to boundary thermal regime in the frame of 2D approach. It simplifies significantly preparation and design of physical experiments with regard to determination of required parameters for experimental setup and to elicitation of the influence of different system parameters, including thermophysical properties of working media. Since the results obtained with the help of the 2D and 3D exact solutions under study are in agreement among themselves and with known

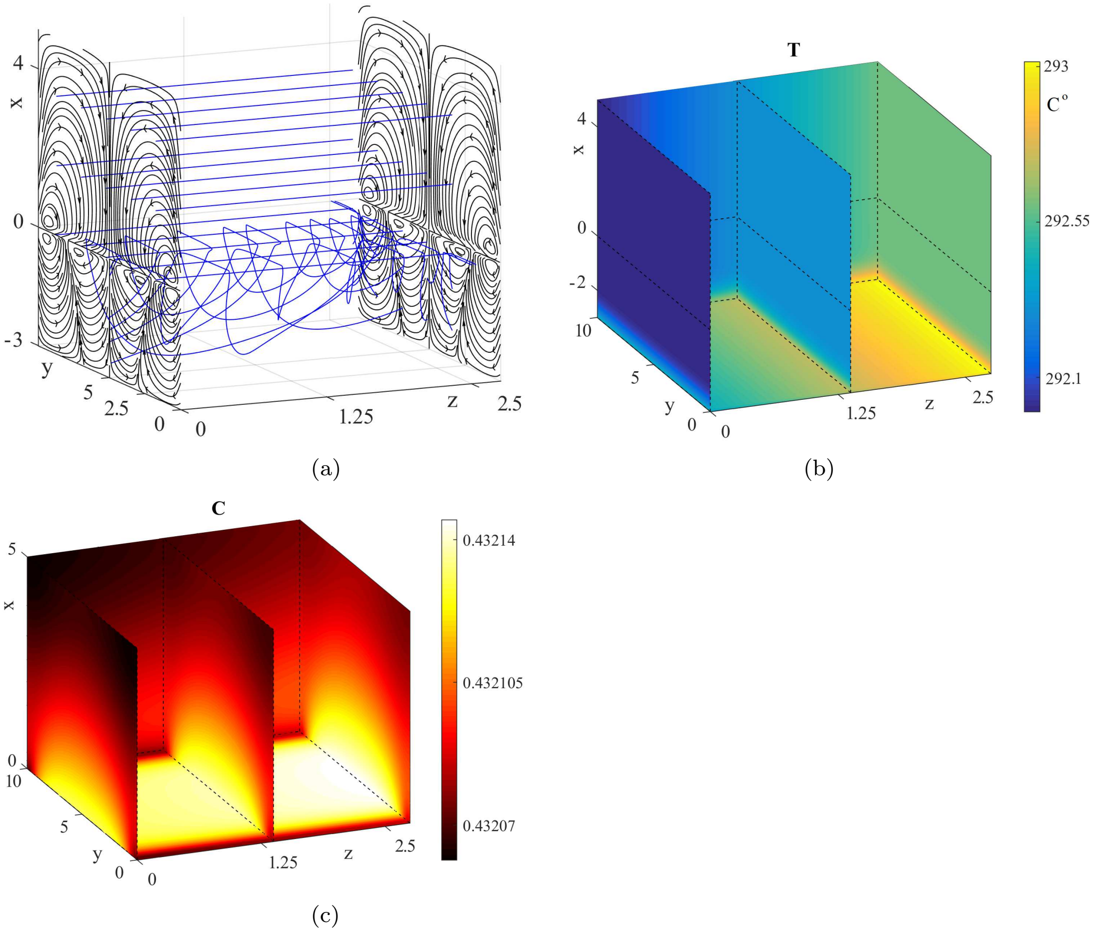

Fig. 6 Streamlines and trajectories (a), temperature (c) and vapor concentration (e) in the system being in microgravity ($g = g_0 \cdot 10^{-2}$) with $x_0 = 3$ mm, $A_1 = -5$ K/m

experiment data it is reasonable to expect that characteristics of the stability derived on the basis of the 2D solution for different configurations in [34,36] can be used to define parameters of the control actions which guarantee the stability of the arising flow regimes. Then in solving the stability problem for 2D solution it is much easier to determine the mechanisms suppressing undesirable perturbations.

The main feature of the 3D solution is that it describes appearance of thermocapillary longitudinal shafts observed in the physical experiments [32,33,45] and of different assemblies of convective cells being the elements of a space-periodic structure of the flow. In addition, the spatial size of the cells can be determined depending on the system configuration and parameters of external actions. We use the “cell” term to refer to a pair of adjacent rolls (or shafts with defects) with opposite circulation. The question of what planforms can be observed in real conditions is the part of the general issue of flow feasibility. Once again we stress that the exact solution was obtained without any assumptions relating to the axial symmetry. Let us note that the 3D solution under study allows one to describe a formation of the regimes with a thermocline and with more complex patterns of temperature field like thermal rolls, thermal shafts with a defect (so-called thermal “horns”), thermal “plume” structure [35,37]. Furthermore, the different pattern of the vapor concentration field can be predicted, for example, solutal shafts and concentration “plume” [37].

5 Concluding remarks

Exact solutions of the evaporative convection equations allows one to generalize the Napolitano classification of the two-layer flow types both in 2D and 3D case. This generalization implies consideration of the planform type and of the thermal pattern form realized in a concrete liquid – gas system under certain conditions. A classification regarding the vapor content is not needed since the solution provides the qualitative agreement of the temperature and concentration characteristics, and distribution of the vapor concentration is determined by the temperature.

The two-dimensional analogue of the solution gives adequate description of the hydrodynamic, thermal and concentration characteristics of the regimes of evaporative convection that arise in a two-layer system. The results derived with the help of 2D solution can be used to obtain preliminary evaluations of effective parameters for the system, to specify a dependence of the flow characteristics on the problem parameters and to have a possibility to forecast transient regimes and potential crisis phenomena related to the loss of stability of the basic state of system. The three-dimensional solution allows one to describe complicated motions with different symmetry and competitive roll structures and thermally different flow classes with dissimilar pattern of the temperature field.

Both 2D and 3D solution enable to test different types of boundary conditions for the temperature and vapor concentration functions and to study influence of the boundary regimes on the characteristics of two-layer flows with diffusive type evaporation/condensation in long channels or in the test sections of the fluidic path. Results obtained on the basis of the presented solutions help us to move forward in understanding mechanisms of formation of different regimes in the systems with phase transition.

6 Appendix 1

When constructing the solution the case with the constant evaporation mass flow rate $M = const$ is considered. The deceptively simple case allows one to perform the comparison with the values of M obtained in experiments and presented as trendlines [46].

Note that if the Dufour and Soret effects are taken into account simultaneously in boundary conditions for the temperature and vapor concentration (2.12) and (2.15), then these conditions can be replaced by equalities

$$\frac{\partial T_2}{\partial n} = 0, \quad \frac{\partial C}{\partial n} = 0. \tag{A.1}$$

Due to conditions (A.1) we have $a_2^2 = 0$, $b_2 = 0$ and

$$c_6^2 = -\frac{(x^0)^4}{24}\frac{g}{\nu_2}E_1E_2 - \frac{(x^0)^3}{6}E_2c_1^2 - \\ -\frac{(x^0)^2}{2}E_2c_2^2 - x^0E_2c_3^2,$$

where coefficients E_1, E_2 and B_1 are expressed in the following form:

$$E_1 = \beta_2A+\gamma b_1,\ \ E_2 = \frac{b_1}{D} - \alpha B_1,\ \ B_1 = \frac{DA - \chi_2\delta b_1}{D\chi_2(1-\alpha\delta)}.$$

Continuity conditions for the velocity and temperature (2.11) at the interface result in equalities of coefficients $c_3^1 = c_3^2$, $c_5^1 = c_5^2$.

Parameter a_2^1 is defined by relation $a_2^1 = (A-A_1)/x_0$ owing to linear temperature distribution (2.13) on the lower wall $x = -x_0$.

Heat balance condition (2.8) leads to the following equalities:

$$\begin{aligned} &\kappa_1a_2^1 - \kappa_2a_2^2 - \delta\kappa_2b_2 = 0,\\ &\kappa_1c_4^1 - \kappa_2c_4^2 - \delta\kappa_2c_6^2 = -LM, \end{aligned} \tag{A.2}$$

where the mass flow rate of evaporating liquids is determined by relation $M = -D\rho_2(c_6^2 + \alpha c_4^2)$ obtained from the mass balance equation (2.9). Since $a_2^2 = b_2 = 0$ the first condition in (A.2) implies that $a_2^1 = 0$. Consequently, equality of the temperature gradients on the lower wall and the interface is fulfilled: $A_1 = A$. The second condition in (A.2) allows one to express constant c_4^1:

$$c_4^1 = \frac{LD\rho_2(c_6^2 + \alpha c_4^2)\kappa_2c_4^2 + \delta\kappa_2c_6^2}{\kappa_1}.$$

Condition for saturated vapor concentration (2.10) has as a consequence the relations $b_1 = C_*\varepsilon_*A$ and $c_7^2 = C_*(1+\varepsilon_*c_5^2)$.

Dynamic conditions (2.7) defines correlations between coefficients c_1^1 and c_1^2, c_2^1 and c_2^2:

$$c_2^1 = \rho\nu c_2^2 + \frac{\sigma_TA}{\rho_1\nu_1}, \quad c_1^1 = \rho\nu c_1^2.$$

Notation ρ and ν have been introduced in Subsection 2.2 (see formula $(2.7)'$).

Integration constant c_1^2, c_2^2, c_3^2 are determined as a solution of the equation system obtained from the no-slip conditions on both walls of the channel (2.14) and additional condition (3.10):

$$\begin{aligned} &\frac{x_0^2}{2}\rho\nu c_1^2 - x_0\rho\nu c_2^2 + c_3^2 = \frac{\sigma_TA}{\rho_1\nu_1}x_0 + \frac{g\beta_1A}{6\nu_1}x_0^3,\\ &\frac{(x^0)^2}{2}c_1^2 + x^0c_2^2 + c_3^2 = -\frac{g(x^0)^3}{6\nu_2}E_1,\\ &\frac{(x^0)^3}{6}c_1^2 + \frac{(x^0)^2}{2}c_2^2 + x^0c_3^2 = \frac{Q}{\rho_2} - \frac{(x^0)^4}{24}\frac{g}{\nu_2}E_1. \end{aligned}$$

From knowing c_1^2, c_2^2, c_3^2, constants c_1^1, c_2^1, c_3^1, c_6^2 can be calculated.

Then, constant c_4^2 is defined with the help of condition of zero heat flux on the upper wall $x = x^0$ (the first equality in (A.1)):

$$c_4^2 = -\frac{(x^0)^5}{120}\frac{4g}{\nu_2}B_2E_1 - \frac{(x^0)^4}{24}\frac{g}{\nu_2}B_1E_1 + \\ +\frac{(x_0)^3}{6}B_1c_1^2 - \frac{(x_0)^2}{2}B_1c_2^2.$$

Now value of c_4^1 can be found through known c_6^2 and c_4^2.

And finally, to define constant c_5^1 condition (2.13) is used:

$$c_5^1 = T_{10} + \frac{x_0^5}{120\chi_1}\frac{g\beta_1 A^2}{\nu_1} - \frac{x_0^4}{24\chi_1}Ac_1^1 + \\ + \frac{x_0^3}{6\chi_1}Ac_2^1 - \frac{x_0^2}{2\chi_1}Ac_3^1 + c_4^1 x_0.$$

It allows one to found successively c_5^2 and c_7^2.

The pressure functions p_i are defined up to an additive constants c_8^i. Without loss of generality we can put the constants to be equal to zero.

7 Appendix 2

The physico-chemical parameters of working fluids are presented below in the order {HFE-7100, nitrogen} (or only HFE-7100):

$\rho = \{1.5 \cdot 10^3,\ 1.2\}$ kg/m^3;
$\nu = \{0.38 \cdot 10^{-6},\ 0.15 \cdot 10^{-4}\}$ m^2/s;
$\beta = \{1.8 \cdot 10^{-3},\ 3.67 \cdot 10^{-3}\}$ K^{-1};
$\chi = \{0.4 \cdot 10^{-7},\ 0.3 \cdot 10^{-4}\}$ m^2/s;
$\kappa = \{0.07,\ 0.02717\}$ W/(m·K);
$\sigma_T = 1.14 \cdot 10^{-4}$ N/(m·K);
$D = 0.7 \cdot 10^{-5}$ m^2/s;
$L = 1.11 \cdot 10^5$ W·s/kg;
$C_* = 0.45$;
$\gamma = -0.5$;
$\varepsilon_* = 0.04$ K^{-1};
Dufour coefficient $\delta = 10^{-5}$ K;
Soret coefficient $\alpha = 5 \cdot 10^{-4}$ K^{-1}.

Conflict of Interest: The authors declare that they have no conflict of interest.

Acknowledgements Authors gratefully thank Shefer Ilia A. for the help in the picture processing.

References

1. Lame G., Clapeyron B.P., Memoire sur la solidification par refroidissement d'un globe liquide, Ann. Chem. Phys., **47**, 250–256 (1831)
2. Boltzmann L., Lectures on Gas Theory, Berkeley, CA: Univ. California Press (1964)
3. Stefan J., Uber das Gleichgewicht und die Bewegung, insbesondere die Diffusion von Lzas gemengen, Sitzungsberichte der Kaiserlichen Akademie der Wissenschaften, Wien, 63–124 (1871)
4. Gibbs J.W., On the equilibrium of heterogeneous substances, Trans. Conn. Acad. Arts Sci., **3**, 108–248 (1875)
5. Gibbs J.W., On the equilibrium of heterogeneous substances, Trans. Conn. Acad. Arts Sci., **3**, 343–524 (1878)
6. Hertz H., Uber die Verdimstung der Flüssigkeiten, insbesondere des Quecksilbers, im luftleeren Raume, Ann. Phys. Chem., **253**, 177–200 (1882)
7. Maxwell J.C., Collected Scientific Papers, Cambridge Univ. Press, Cambridge, **2** (1890)
8. Langmuir I., The evaporation, condensation and reflection of molecules and the mechanism of adsorption, Phys. Rev., **8(2)**, 149–176 (1916)
9. Knudsen M., Die maximale Verdampfungsgeschwindigkeit des Quecksilbers, Ann. Phys. Chem., **47**, 697–708 (1915)
10. Kutateladze S.S., Teploperedacha pri kondensatsii i kipenii (Heat Transfer under Condensation and Boiling), MashGiz, Moscow, Leningrad (1952) [in Russian]
11. Kutepov A.M., Sterman L.S., Styushin N.G., Gidrodinamika i teploobmen pri paroobrazovanii (Hydrodynamics and heat transfer by vaporization) Vysshaya shkola, Moscow (1986) [in Russian]
12. Kutateladze S.S., Osnovy teorii teploobmena (Basics of the heat transfer theory), Atomizdat, Moscow (1979) [in Russian]
13. Knake O., Stranskii I.N., Mechanism of evaporation, Usp. Fiz. Nauk, **68(2)**, 261–305 (1959) [in Russian]
14. Sterman L.S., On the theory of heat emission under liquid boiling, Zh. Tekh. Fiz., **23(2)**, 341–351 (1953) [in Russian]
15. Isachenko M.R., Teploobmen pri kondensatsii (Heat Transfer under Condensation), Energiya, Moscow (1977) [in Russian]
16. Prosperetti A., Boundary conditions at a liquid-vapor interface, Meccanica, **14(1)**, 34–47 (1979)
17. Margerit J., Colinet P., Lebon G., Iorio C.S., Legros J.C. Interfacial nonequilibrium and Benard – Marangoni instability of a liquid- vapor system, Phys. Rev. E., **68**, 041601 (2003)
18. Haut B., Colinet P., Surface-tension-driven instability of a liquid layer evaporating into an inert gas, J. Colloid Interface Sci., **285**, 296–305 (2005)
19. Das K.S., Ward C.A., Surface thermal capacity and its effects on the boundary conditions at fluid-fluid interfaces, Phys. Rev. E, **75**, 065303 (2007)
20. Bratukhin Yu.K., Makarov S.O., Mezhfaznaya konvektsiya (Interphase Convection), Perm State Univ., Perm (1994) [in Russian]
21. Iorio C.S., Goncharova O.N., Kabov O.A., Heat and mass transfer control by evaporative thermal pattering of thin liquid layers, Comput. Therm. Sci., **3(4)**, 333–342 (2011)
22. Goncharova O.N., Simulation of flows under the conditions of heat and mass transfer at interface, Izv. Altai. Gos. Univ., **73(1/2)**, 12–18 (2012) [in Russian]
23. Bekezhanova V.B., Goncharova O.N., Problems of Evaporative Convection (Review), Fluid Dynamics, **53(1)**, S69–S102 (2018)
24. Ovsyannikov, L. V., Groups and invariant-group solutions of differential equations, Dokl. Akad. Nauk SSSR, **118(3)**, 439–442 (1958) [in Russian]
25. Andreev V.K., Kaptsov O.V., Pukhnachov V.V., Rodionov A.A., Applications of group theoretical methods in hydrodynamics, 408. Kluwer Academic Publ., Dordrecht, Boston, London (1998)
26. Shliomis M.I., Yakushin V.I., Convection in a two-layers binary system with an evaporation, Collected papers: Uchenye zapiski Permskogo Gosuniversiteta, seriya Gidrodinamika, **4**, 129–140 (1972) [in Russian]
27. Goncharova O.N., Rezanova E.V., Example of an exact solution of the stationary problem of two-layer flows with evaporation at the interface, J. Appl. Mech. Techn. Phys., **55(2)**, 247–257 (2014)
28. Goncharova O.N., Kabov O.A., Investigation of the two-layer fluid flows with evaporation at interface on the basis of the exact solutions of the 3D problems of convection, Journal of Physics: Conference Series, **754**, 032008 (2016)

29. Katkov, V.L., Precise solutions of some convection problems, Prikl. Mat. Mekh., **32(3)**, (1968) 482–487.
30. Pukhnachov V.V., Group-theoretical nature of the Birikh's solution and its generalizations, Book of Proc. Symmetry and differential equations, Krasnoyarsk, 180–183 (2000) [in Russian]
31. Lyulin, Y.V. and Kabov, O.A., Evaporative convection in a horizontal liquid layer under shear-stress gas flow, Int. J. Heat Mass Transfer, **(70)**, 599–609 (2014).
32. Lyulin, Yu.V., Feoktistov, D.V., Afanas'ev, I.A., et al., Measuring the rate of local evaporation from the liquid surface under the action of gas flow, Tech. Phys. Lett., **41(7)**, 665–667 (2015).
33. Kreta A., Lyulin Y., Kabov O., Effect of temperature on the convection flow within the liquid evaporation into the gas flow, J. Phys.: Conf. Ser., **754**, 032011 (2016)
34. Bekezhanova V.B., Goncharova O.N., Stability of the exact solutions describing the two-layer flows with evaporation at interface, Fluid Dyn. Res., **48(6)**, 061408 (2016)
35. Bekezhanova V.B., Goncharova O.N. Modeling of three dimensional thermocapillary flows with evaporation at the interface based on the solutions of a special type of the convection equations, Appl. Math. Model., **62**, 145–162 (2018)
36. Bekezhanova V.B., Shefer I.A. Influence of Gravity on the Stability of Evaporative Convection Regimes, Microgravity Sci. Tech., **30(4)**, 543–560 (2018)
37. Bekezhanova V.B., Goncharova O.N., Thermocapillary convection with phase transition in the 3D channel in a weak gravity field, Microgravity Sci. Tech., in Press (2019)
38. Sivukhin D.V., General Physics Course, Vol. 2. Fizmatlit, Moscow (2005) [in Russian]
39. Goncharova O.N., Rezanova E.V., Lyulin Yu.V., Kabov O.A., Analysis of a convective fluid flow with a concurrent gas flow with allowance for evaporation, High Temperature, **55(6)**, 887–897 (2017)
40. Dyagel D.V., Rezanova E.V. Mathematical modeling of flows with evaporation in a two-layer system with a thermally insulated upper boundary, Izv. Altai. Gos. Univ., **96(4)**, 94–97 (2017) [in Russian]
41. Napolitano L.G., Plane Marangoni- Poiseuille two immiscible fluids, Acta Astronaut., **7**, 461–478 (1980)
42. Bekezhanova V.B., Goncharova O.N., Rezanova E.V., Shefer I.A., Stability of two-layer fluid flows with evaporation at the interface, Fluid Dyn., **52(2)**, 189–200 (2017)
43. Bekezhanova V.B., Goncharova O.N., Shefer I.A., Analysis of an exact solution of problem of the evaporative convection (Review). Part I. Plane case, J. Siberian Federal Univ. Math. and Phys., **11(2)**, 178–190 (2018)
44. C.R.C. Weast, Handbook of Chemistry and Physics. CRC Press Inc., Boca Raton, Florida, 1979
45. Bekezhanova V.B., Kabov O.A., Influence of internal energy variations of the interface on the stability of film flow, Interfacial Phenomena and Heat Transfer, **4(2-3)**, 133-156 (2016)
46. Goncharova O.N., Rezanova E.V., Lyulin Yu.V., Kabov O.A., Modeling of two-layer liquid-gas flow with account for evaporation, Thermophysics and Aeromechanics, **22(5)**, 631–637 (2015)